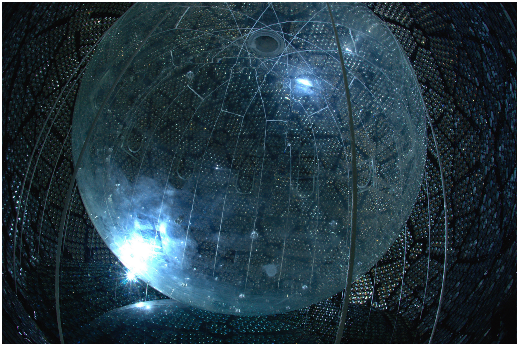

Inside of **SNO+ detector**, *cavity water fill, May 2014*

Geoneutrinos

Physics and Prospects

Joachim Rose
University of Liverpool

February 2017

Overview

- Neutrino **geophysics**
- Geoneutrino **detections**
- **SNO+ detector**
  - neutrinoless double-beta decay
  - current status
- Geoneutrino **flux prediction**
- SNO+ first results (not yet)
- Future **prospects**

"Geoneutrinos reveal Earth's inner secrets"

Nature, v 436, p 499, July 2005 : Experimental investigation of geologically produced antineutrinos with KamLAND.

Neutrino Geophysics

Present day volcanism and Earth magnetic field

Heat loss estimates

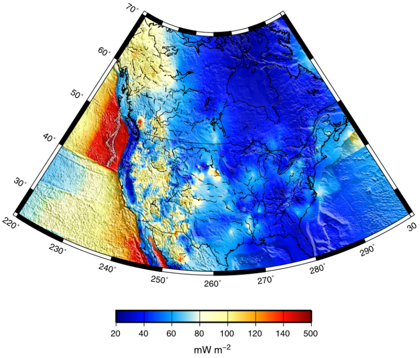

Global heat losses estimates:

- Present day 41 - 47 TW
- Average of 74 - 83 mW/m^2

Table 1
Estimates of the continental and oceanic heat flux and global heat loss.

	Continental (mW m^{-2})	Oceanic (mW m^{-2})	Total (TW)
Williams and von Herzen (1974)	61	93	43
Davies (1980)	55	95	41
Sclater et al. (1980)	57	99	42
Pollack et al. (1993)	65	101	44
Jaupart et al. (2007)[a]	65	94	46

[a] The average oceanic heat flux does not include the contribution of hotspots. The total heat loss estimate includes 3 TW from oceanic hotspots.

Why has the planet interior **not** cooled down entirely over the last few Gy?

[1] Map from Mareschal, Jaupart, Tectonophysics 609 (2013) 524-534.
[2] Table from J.-C. Mareschal et al., Journal of Geodynamics 54 (2012) 43-54.

Earth radiogenic heating

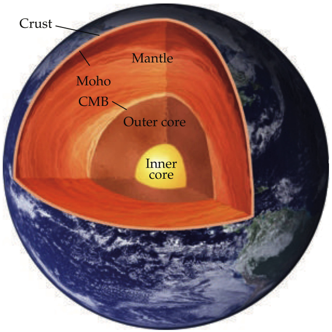

Image from doi:10.1155/2012/235686

Heat sources, surface losses[1]

Earth core [2]	5 - 10 TW
Radioactivity (K,Th,U)	17 - 23 TW
Tidal dissipation	0.1 TW
Crust (grav. energy)	0.3 TW
Mantle cooling[3]	8 - 29 TW
Surface heat losses	43 - 49 TW

Radiogenic heat per decay chain[4]

$$^{238}\mathrm{U} \rightarrow {}^{206}\mathrm{Pb} + 8\alpha + 6\mathrm{e} + 6\bar{\nu}_e + 51.698\,\mathrm{MeV}$$

$$^{235}\mathrm{U} \rightarrow {}^{207}\mathrm{Pb} + 7\alpha + 4\mathrm{e} + 4\bar{\nu}_e + 46.402\,\mathrm{MeV}$$

$$^{232}\mathrm{Th} \rightarrow {}^{208}\mathrm{Pb} + 6\alpha + 4\mathrm{e} + 4\bar{\nu}_e + 42.652\,\mathrm{MeV}$$

$$^{40}\mathrm{K} \rightarrow {}^{40}\mathrm{Ca} + \mathrm{e} + \bar{\nu}_e + 1.311\mathrm{MeV}(89.3\%)$$

$$^{40}\mathrm{K} + \mathrm{e} \rightarrow {}^{40}\mathrm{Ar} + \nu_e + 1.505\,\mathrm{MeV}(10.7\%)$$

[1] C. Jaupart et al., Treatise on Geophysics: Temperatures, Heat and Energy in the Mantle of the Earth, 2007
[2] Core cooling, latent heat, gravitational energy due to chemical separation.
[3] Present day mantle cooling rate of 53 - 190 K Gy^{-1}
[4] S. Dye, Reviews of Geophysics, 50, RG3007, 2012

Abundance estimates for K, Th and U

Table 2: Abundance estimates of U, Th, and K in BSE and DM. Uncertainties are included where available.

U (ppb)	Th (ppb)	K (ppm)	Th/U	K/U	Power (TW)	Reference
Bulk silicate Earth (BSE)						
Collisional erosion model						
10	38	120	3.8	12000	9.6	O'Neill and Palme [62]
Based on enstatite chondrites						
13.5	41.7	385	3.1	28500	15	Javoy [63]
12.1	49.2	146	3.5	12000	11	Javoy et al. [64]†
Based on terrestrial rocks and C1 carbonaceous chondrite ratios of RLE abundances						
20.8	79.0	264	3.8	12700	20	Hart and Zindler [58]
20.3 ± 20%	79.5 ± 15%	240 ± 20%	3.9	11800	20 ± 4	McDonough and Sun [55]
21.8 ± 15%	83.4 ± 15%	260 ± 15%	3.8	11900	21 ± 3	Palme and O'Neill [59]
17.3 ± 3.0	62.6 ± 10.7	190 ± 40	3.6	11000	16 ± 3	Lyubetskaya and Korenaga [61]
20 ± 4	80 ± 12	280 ± 60	4.0	13800	20 ± 4	Arevalo et al. [60]
Based on energetics of mantle convection ("conventional" scaling)						
31	124	310	4.0	10000	30	Turcotte and Schubert [65]
Depleted mantle (DM)—MORB source						
3.2 ± 0.5	7.9 ± 1.1	50	2.5	15600	2.8 ± 0.4*	Workman and Hart [66]
4.7 ± 30%	13.7 ± 30%	60 ± 28%	2.9	12800	4.1 ± 1.2*	Salters and Stracke [67]
8 ± 20%	22 ± 20%	152 ± 20%	2.8	19000	7.5 ± 1.5*	Arevalo and McDonough [68]

†Model of Javoy et al. [64] is constructed following Javoy's recipe as described in [69]. *Calculation of radiogenic power for DM estimates assumes that the entire mantle has DM composition.

Assumptions made to predict K, Th and U abundances:

- Stone meteorite **chondrules** originate from solar nebula at **planet formation**
- Earth is a **dynamic system**; initial uniform abundances have changed
  - Crust : high abundances
  - Mantle : depleted, low abundances
  - Core : assumed zero

[1] Table from Review Article, *Geoneutrinos*, Advances in High Energy Physics (2012)

More about chondrites

Chondrites:

- Stony (non-metallic) meteorites
- Formed from dust and small grains in the **early solar system**
- **Not been modified**; no melting or differentiation of the parent body
- Contain small, colourful, grain-like inclusions known as "chondrules"
- Most **common** of meteorite, 86 % of total found

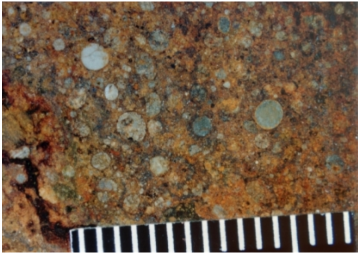

[1] Definitions and images: see https://en.wikipedia.org/wiki/Chondrite.

Chondrites not representative of early solar nebula

SNO

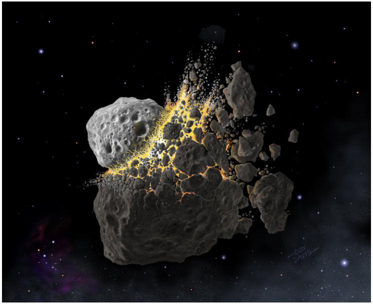

nature astronomy | LETTERS

PUBLISHED: 23 JANUARY 2017 | VOLUME: 1 | ARTICLE NUMBER: 0035

Rare meteorites common in the Ordovician period

Philipp R. Heck[1,2]*, Birger Schmitz[1,3], William F. Bottke[4], Surya S. Rout[1,2], Noriko T. Kita[5], Anders Cronholm[3], Céline Defouilloy[5], Andrei Dronov[6,7] and Fredrik Terfelt[3]

Most meteorites that fall today are H and L type ordinary chondrites, yet the main belt asteroids best positioned to deliver meteorites are LL chondrites[1,2]. This suggests that the current meteorite flux is dominated by fragments from recent asteroid breakup events[3,4] and therefore is not representative over longer (100-Myr) timescales. Here we present the first reconstruction of the composition of the background meteorite flux to Earth on such timescales. From limestone that formed about one million years before the breakup of the L-chondrite parent body 466 Myr ago, we have recovered relict minerals from coarse micrometeorites. By elemental and oxygen-isotopic analyses, we show that before 466 Myr ago, achondrites from different asteroidal sources had similar or higher abundances than ordinary chondrites. The primitive achondrites, such as lodranites and acapulcoites, together with related ungrouped achondrites, made up ~15–34% of the flux compared with only ~0.45% today. Another group of abundant achondrites may be linked to a 500-km cratering event on (4) Vesta that filled the inner main belt with basaltic fragments a billion years ago[5]. Our data show that the meteorite flux has varied over geological time as asteroid disruptions create new fragment populations that then slowly fade away from collisional and dynamical evolution. The current flux favours disruption events that are larger, younger and/or highly efficient at delivering material to Earth.

from the LCPB that might have arrived on Earth before should have even shorter exposure ages. This indicates that a sample separation of one million years before the strata containing the first abundant L chondrites is large enough to assess the pre-LCPB flux. The interval sampled represents a time average of about 10 to 100 kyr and was selected with the aim of determining whether the composition of the meteorite flux to Earth was similar to or different from that of today. This is the first reconstruction of the background flux of the different meteorite types in a geological time perspective. Similar reconstructions are ongoing for other periods in the Earth's geological past[10].

The presence of surface-implanted solar-wind-derived helium and neon in sediment-dispersed extraterrestrial chrome spinels (SECs) that were recovered from similar sediments from several younger Ordovician beds from sites in Sweden, China and Russia is evidence that the SECs were parts of micrometeorites[11–13]. Because the abundance ratio of the two ordinary chondrite groups H and L chondrites in recently fallen coarse micrometeorites[14,15] is similar to this ratio in macroscopic meteorites, micrometeorites bearing coarse chromite grains can be used as a proxy for meteorites[7]. The same consistency between the composition of coarse micrometeorites and meteorites has been documented based on fossil material for the Ordovician period after the LCPB[8]. This relation is useful because of the much higher abundance of SECs compared with fossil meteorites[6], allowing analyses of a larger number of samples[7].

We recovered 46 chrome-spinel grains with diameters >63 μm,

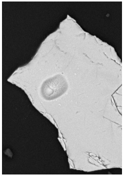

"From limestone that formed about one million years before the breakup of the L-chondrite parent body 466 Myr ago, we have recovered relict minerals from coarse micrometeorites. By elemental and oxygen-isotopic analyses, we show that **before 466 Myr ago**, **achondrites** from **different asteroidal sources** had **similar or higher abundances** than ordinary chondrites."

[1] Illustration Don Davis, Southwest Research Institute. New York Times, 23 Jan 17.

Time evolution of elemental abundance

Earth as a **dynamical system** over long (Gy) time scales

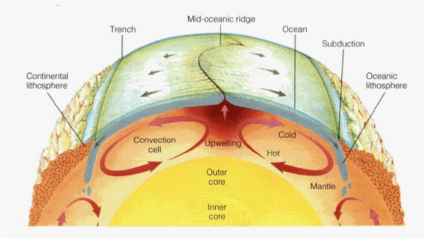

Goldschmidt classification in the periodic table

Period \ Group	1	2	3	4	5	6	7	8	9	10	11	12	13	14	15	16	17	18
1	1 H																	2 He
2	3 Li	4 Be											5 B	6 C	7 N	8 O	9 F	10 Ne
3	11 Na	12 Mg											13 Al	14 Si	15 P	16 S	17 Cl	18 Ar
4	19 K	20 Ca	21 Sc	22 Ti	23 V	24 Cr	25 Mn	26 Fe	27 Co	28 Ni	29 Cu	30 Zn	31 Ga	32 Ge	33 As	34 Se	35 Br	36 Kr
5	37 Rb	38 Sr	39 Y	40 Zr	41 Nb	42 Mo	43 Tc	44 Ru	45 Rh	46 Pd	47 Ag	48 Cd	49 In	50 Sn	51 Sb	52 Te	53 I	54 Xe
6	55 Cs	56 Ba	*	72 Hf	73 Ta	74 W	75 Re	76 Os	77 Ir	78 Pt	79 Au	80 Hg	81 Tl	82 Pb	83 Bi	84 Po	85 At	86 Rn
7	87 Fr	88 Ra	**	104 Rf	105 Db	106 Sg	107 Bh	108 Hs	109 Mt	110 Ds	111 Rg	112 Cn	113 Nh	114 Fl	115 Mc	116 Lv	117 Ts	118 Og

*	57 La	58 Ce	59 Pr	60 Nd	61 Pm	62 Sm	63 Eu	64 Gd	65 Tb	66 Dy	67 Ho	68 Er	69 Tm	70 Yb	71 Lu
**	89 Ac	90 Th	91 Pa	92 U	93 Np	94 Pu	95 Am	96 Cm	97 Bk	98 Cf	99 Es	100 Fm	101 Md	102 No	103 Lr

Goldschmidt classification: Lithophile Siderophile Chalcophile Atmophile Synthetic

Goldschmidt classification: **Lithophile elements** (including K, Th and U) remain on or close to the **surface** by forming compounds with oxygen that do **not sink** into the core.

[1] Image Byrd Polar Research Center, Ohio State University
[2] Periodic table Wikipedia, Goldschmidt classification.

Elemental abundance

Example USGS map of Uranium concentration on or near surface

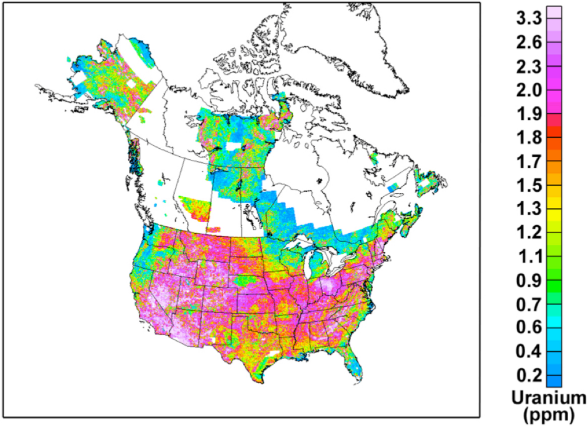

Geophysics reference model

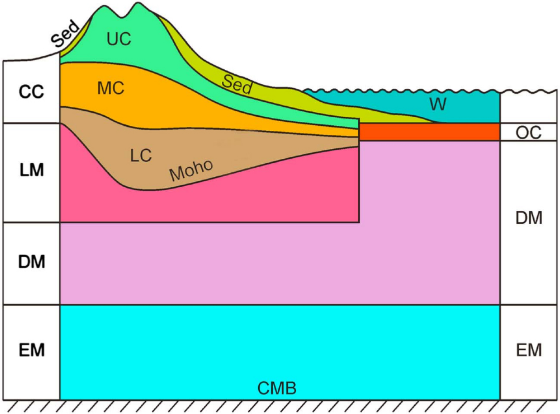

Huang et al. (2013), *A reference Earth model for the heat-producing elements and associated geoneutrino flux,* Geochem. Geophys. Geosyst., 14, 2003-2029.

Geophysics reference model, geoneutrino flux prediction

SNO+

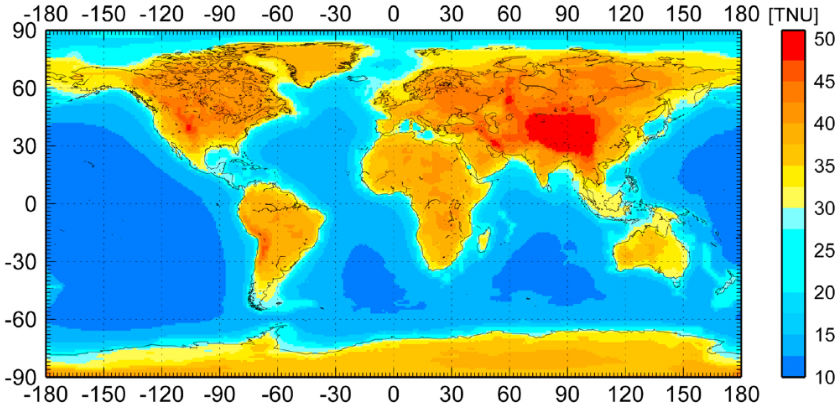

Huang et al. (2013), *A reference Earth model for the heat-producing elements and associated geoneutrino flux,* Geochem. Geophys. Geosyst., 14, 2003-2029.

Geoneutrino flux predictions

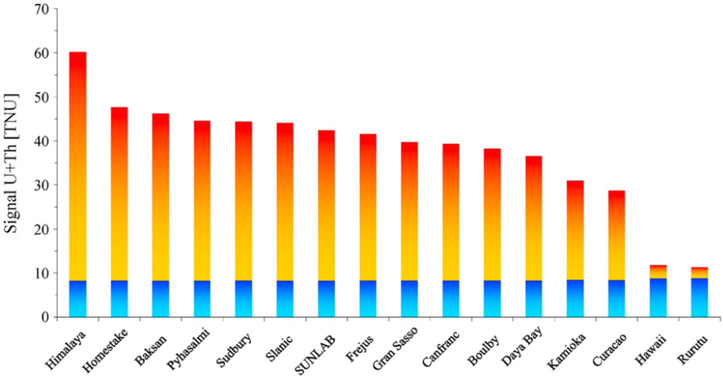

Huang et al. (2013), *A reference Earth model for the heat-producing elements and associated geoneutrino flux,* Geochem. Geophys. Geosyst., 14, 2003-2029.

Geoneutrino Detections

Reactor anti-neutrinos

Cowan and Reines, Savannah River reactor, 1955

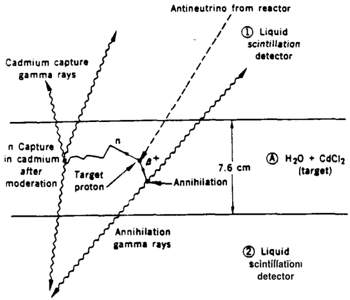

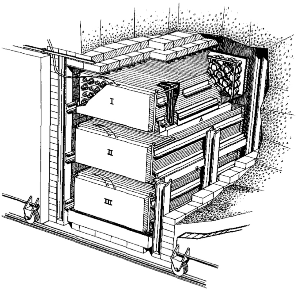

600 kg water target (tank A and B), distance 11 m from reactor, 600 MW.

A geoneutrino (anti-neutrino) background?

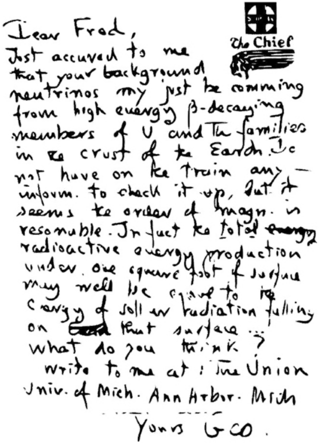
The Chief

Dear Fred,
Just occured to me that your background neutrinos my just be comming from high energy β-decaying members of U and Th families in the crust of the Earth. I do not have on the train any information to check it up, but it seems the order of magn. is resonable. In fact the total radioactive energy production under one square foot of surface may well be equal to the energy of soll[ar] radiation falling on that surface...
what do you think?
write to me at: The Union Univ. of Mich. Ann Arbor. Mich
Yours GG.

While onboard of the SantaFe Chief Train, Georg Gamow wrote to Fred Reines (see left):

> *It just occurred to me that your* **background** *may just be coming from* **high energy beta-decaying members of U and Th families** *in the* **crust** *of the Earth.*

The **first estimate of geo-neutrino flux** was given in a teletype message by Reines in response to the letter of Gamow:

> *Heat loss from Earth's surface is 50 erg* $\mathrm{cm}^{-2}\ \mathrm{s}^{-1}$*. If assume all due to beta decay than have only enough energy for about* 10^8 *one-MeV neutrinos* cm^{-2} *and s.*

[1] From G. Fiorentini et al., Physics Reports 453 (2007) 117-172.

KamLAND 2005

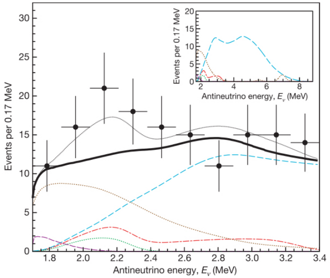

Figure 3 | $\bar{\nu}_e$ energy spectra in KamLAND. Main panel, experimental points together with the total expectation (thin dotted black line). Also shown are the total expected spectrum excluding the geoneutrino signal (thick solid black line), the expected signals from ^{238}U (dot-dashed red line) and ^{232}Th (dotted green line) geoneutrinos, and the backgrounds due to reactor $\bar{\nu}_e$ (dashed light blue line), ^{13}C$(\alpha,n)^{16}$O reactions (dotted brown line), and random coincidences (dashed purple line). Inset, expected spectra extended to higher energy. The geoneutrino spectra are calculated from our reference model, which assumes 16 TW radiogenic power from ^{238}U and ^{232}Th. The error bars represent ± 1 standard deviation intervals.

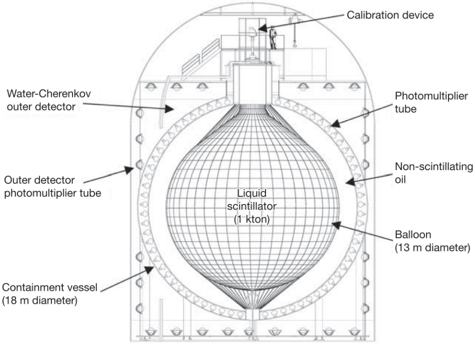

"Assuming a Th/U mass concentration ratio of 3.9, the 90 percent confidence interval for the total number of geoneutrinos detected is 4.5 to 54.2. This result is consistent with the central value of 19 predicted by geophysical models."

[1] NATURE, Vol 436, 28 July 2005

Borexino 2015

Gran Sasso National Laboratory, Italy
278 tons of organic liquid scintillator
Estimated anti-neutrino **background** < 0.65 **events** (90% CL)
Data from 2007 to 2015, total of **2055.9 days** before cuts

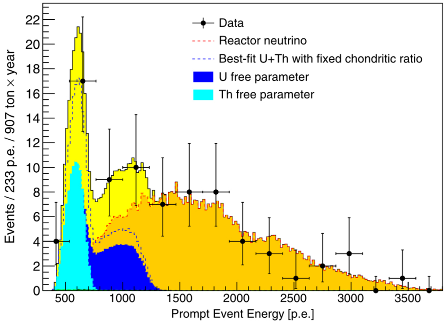

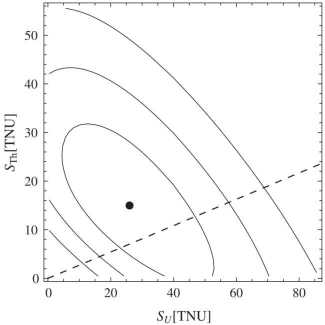

$$S_{geo} = 23.7^{+6.5}_{-5.7}\,(\text{stat})^{+0.9}_{-0.7}\,(\text{sys})\text{ events}$$
$$= 43.5^{+11.8}_{-10.4}\,(\text{stat})^{+2.7}_{-2.4}\,(\text{sys})\ \mathrm{TNU}$$

[1] Physical Review D 92, 031101(R) (2015)

KamLAND 2013 anti-neutrino results

Total detector live time of **2991 days**, 2002 to 2012.

From mid-2007 onwards liquid scintillator (^{210}Po) purification

$^{13}C\ (\alpha, n)\ ^{16}O$ **background reduced by factor 20**

Fukushima accident, March 2011, **reactor shutdown**

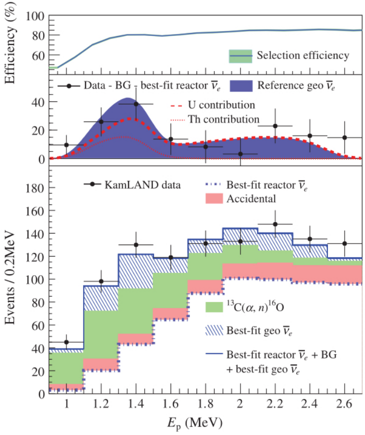

Geoneutrino flux

$$S_{geo} = (3.4 \pm 0.8) \cdot 10^6 \mathrm{cm}^{-2} \mathrm{s}^{-1}$$

Total radiogenic heat production

$$P_{rad} = 11.2^{+7.9}_{-5.1}\ \mathrm{TW}$$

(Th/U abundance ratio 3.9/1)

[1] Physical Review D 88, 033001 (2013)

SNO+ Detector

SNO+ Collaboration

					
Queen's Univ. Laurentian Univ. Univ. of Alberta TRIUMF SNOLAB	BNL, AASU, Penn., UNC, U Washington, UC Berkley/LBNL Chicago, UC Davis	Oxford Sussex Lancaster Liverpool QMUL	TU Dresden	LIP Lisboa LIP Coimbra	UNAM

Previous SNO solar neutrino experiment - until 2006

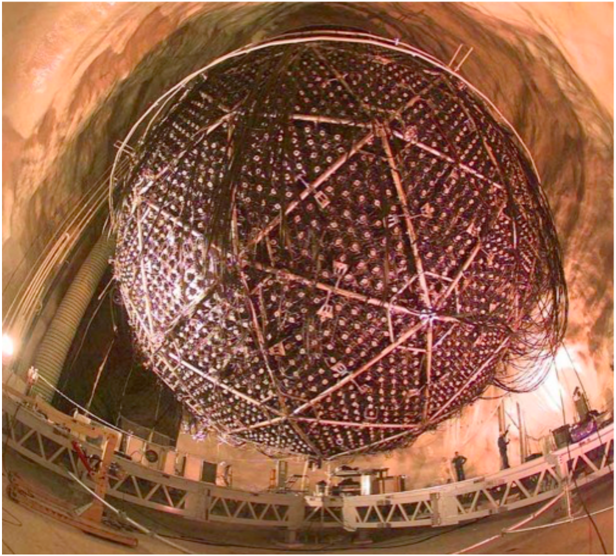

SNO detector cavern, wide angle 'fisheye' view

SNO+ detector characteristics

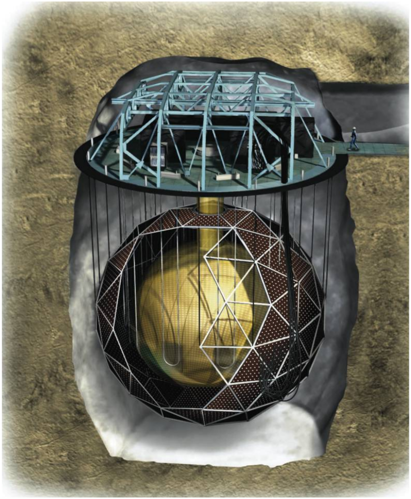

SNO detector, image National Geographic

- Conversion of SNO to search for neutrinoless double beta-decay
- 12 m diameter acrylic vessel
- 780 tons liquid scintillator
- Tellurium loaded into scintillator
  2340 kg Te at 0.3% loading
- Surrounded by $\approx$ 9500 PMT
  18 m diameter support structure
- 1700 tonnes water inner shielding
  5300 tonnes water outside
- Cavern Urylon liner radon seal, anti-radon cover gas layer
- Location Sudbury, Ontario, Canada
- Depth 2092 m below surface
  6010 m water equivalent

Detector conversion into SNO+

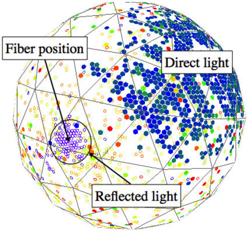

Fibre coupled LED light pulse event

Telluric acid, underground storage

- install underground liquid scintillator plant ✓
- add an acrylic vessel hold-down mechanism ✓
- repair, i.e. PMT bases, cavity floor liner ✓
- upgrade the data acquisition, trigger, electronics ✓
- improve the cover gas radon exclusion✓
- change the calibration source manipulator ✓
  prepare new radioactive calibration sources ✓
- new fibre coupled LED calibration system ✓
- new simulation and event reconstruction codes ✓
- develop technique for tellurium loading ✓
- acquire tellurium acid, store underground ✓
- raise both cavern and acrylic vessel water levels ✓
- fill with (pure or Te loaded) scintillator

Neutrinoless double beta-decay

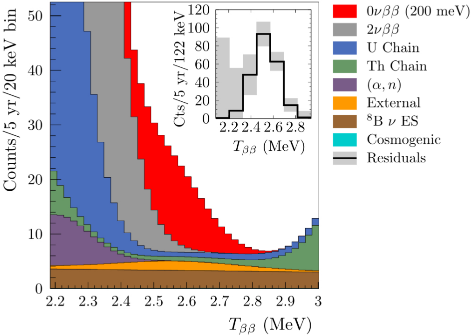

Envisaged detector operation sequence:

- Short initial water fill, compare against SNO performance
- Short liquid scintillator fill, background verification (first **geoneutrino data**)
- Long **tellurium loaded scintillator phase(s)** (**geoneutrino data**)
  - Phase I, 0.3 % loading, five years: 55 - 133 meV effective neutrino mass
  - Phase II, 3 % loading, high QE PMT: 19 - 46 meV effective neutrino mass

[1] S. Andringa et al., Advances in High Energy Physics, Volume 2016, Article ID 6194250

Geoneutrino observations

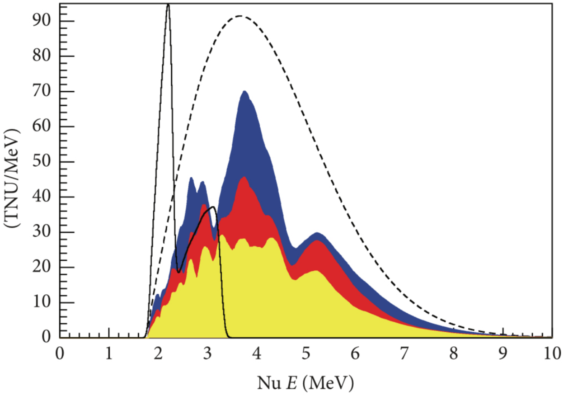

Low background of < 1 event per year, **low reactor neutrino flux**

- SNO+ deeper (2000 m) than Borexino, KamLAND, less external neutron flux
- (α, n) process suppressed, scintillator recirculation system

High event rate ~ 30/year, 780 tons (SNO+) vs 278 tons (Borexino) target mass

[1] S. Andringa et al., Advances in High Energy Physics, Volume 2016, Article ID 6194250

Geoneutrino Flux Prediction

Why yet another geoneutrino rate (spectrum) calculation?

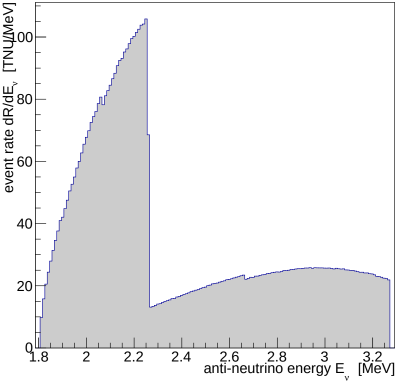

Geoneutrino inverse beta-decay event rate

- Energy spectrum (or spectra) are necessary input for detector simulation and data analysis
- Which effects change the **shape** of the energy spectrum?
- Correct neutrino survival probability?
- Expected inverse beta-decay event rate at SNO+ location

$$R = 39.2\ \mathrm{TNU}$$

For a specific chosen set of assumptions[1], i.e. thorium and uranium abundances.

[1] S. T. Dye, Earth and Planetary Science Letters 297 (2010) 1-9

Geoneutrino flux prediction

SNO+

$$\frac{d\phi_i(\vec{R})}{dE_{\bar{\nu}}} = \int dV \, \frac{\rho(\vec{r})}{4\pi|\vec{R}-\vec{r}|^2} \cdot \frac{a_i(\vec{r})C_i}{\tau_i m_i} \cdot f_i(E_{\bar{\nu}}) \cdot \mathbf{P_s}(E_{\bar{\nu}}, \vec{r}, \vec{R}, n_e(\vec{r}'))$$

- Adaptive Monte Carlo volume integration (GSL/FGSL, Vegas)
- Earth model: Crust 2.0 and PREM (layer depth, density)
- Thorium and uranium abundances as in Dye (2010)
- Th and U decay chains (rates, energy spectra) as in Fiorentini (2007)[2]
- Neutrino **survival probability** calculation : new code
    - **three** mass eigenstates neutrino oscillation
    - electron-neutrino interaction potential **(matter effect)**
    - **varying** electron number density $\mathbf{n_e}(\vec{r}')$ along neutrino path $\vec{r}'$
- Oscillation parameters: Forero et al., Physical Review D 90 (2014)

[2] Fiorentini, Lissia, Mantovani, Physics Reports 453 (2007)

Continental vs oceanic crust, elevation

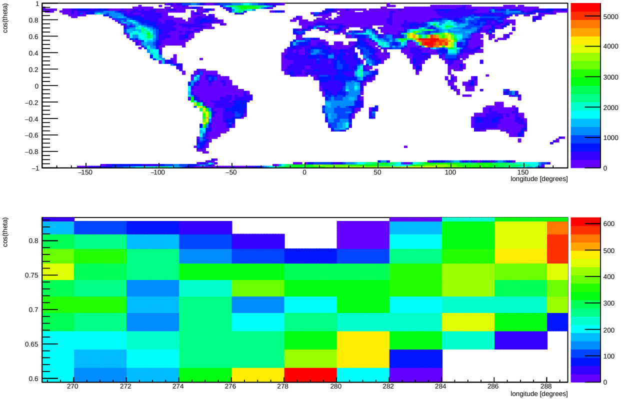

- Crust 2.0 model
- select continental (oceanic) crust by **elevation** only
- predicted SNO+ rate : 39.8 TNU
- compare with 39.2 TNU, Dye (2010)

Select continental (oceanic) crust by elevation and thickness

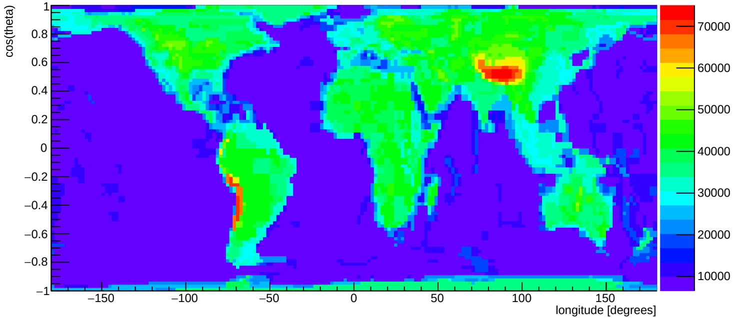

- Crust 2.0 model
- add all tiles of **crust thickness** > 15 km to continental crust
- new predicted SNO+ rate : **41.5 TNU**
- previously, select by elevation only, rate was 39.8 TNU

Survival probability, for three neutrino states, with matter effect

SNO+

$$\imath\,\hbar\frac{d}{dt}|\,\nu(t)> \;=\; \left[\frac{1}{2E_\nu}\,\mathbf{U}^\dagger\begin{pmatrix}0 & 0 & 0\\ 0 & \Delta m^2_{21} & 0\\ 0 & 0 & \Delta m^2_{31}\end{pmatrix}\mathbf{U}+\begin{pmatrix}\mathbf{V(t)} & 0 & 0\\ 0 & 0 & 0\\ 0 & 0 & 0\end{pmatrix}\right]|\,\nu(t)>$$

$$V(t) \;=\; \sqrt{2}\cdot G_F\cdot n_e(\,\vec{r}(t)\,)$$

New numerical code:[3]

- Break neutrino path into (many) **steps of constant matter density**
- For each step solve equation numerically (eigenvalue problem)
- Compare numerical values (LAPACK95) against analytical solution
- Checks against known special cases (exponential, constant, zero density)
- Similar to GLoBES (ν beams), **optimised** for Earth volume integration
- Also run as parallel calculations on a GPU, **speedup** $\sim$ 100 times

[3] R. Fair, S. Hussain, B. Mawdsley, Final year projects, Liverpool, 2014/15

Neutrino survival probability

Frequently made approximation:

$$P_s \approx 1 - sin^2(2\theta_{12}) \cdot \sin^2(1.27\Delta m^2_{12} \frac{L}{E}) \approx 0.56 \pm 0.02$$

Full calculation with three neutrinos, matter effect, Earth volume average:

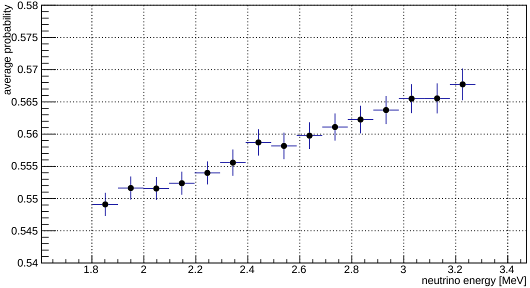

- Errors shown are due to numerical integration over volume.
- There is an (expected) change of survival probability with energy.
- Small effect relative to the overall error due to $sin^2(2\theta_{12})$.

Uncertainty of neutrino oscillation parameter estimates

Visualisation of Nu-Fit 2.0 $\Delta\chi^2$ data, JHEP 11 (2014) 052, arXiv:1409.5439

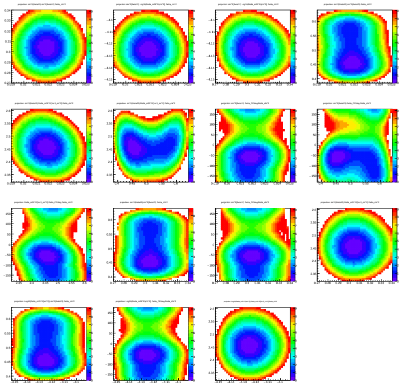

- Six oscillation parameters
- 15 possible pairs
- Selected pairs $(\sin^2(\theta_{13}), \sin^2(\theta_{12}))$, $(\sin^2(\theta_{23}), \Delta m^2_{31})$, $(\Delta m^2_{21}, \delta_{CP})$
- Turn $\Delta\chi^2(x, y)$ into probability $P(x, y)$
- Generate random (x_i, y_i) pairs
- Re-run geoneutrino calculation
- Study variations in predicted rate

Oscillation parameter uncertainty

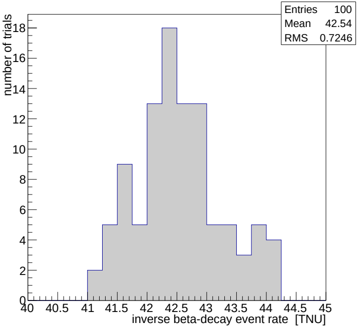

- Repeat calculation with sets of random oscillation parameter values
- Equal probability of each trial, consistent with $\Delta\chi^2$ distributions
- The predicted inverse beta-decay rate is (42.5 ± 0.8) TNU
- Appears to be a **change in rate of $+1$ TNU**
- **False alarm**! See next slide.

Change in event rate vs $\sin^2(\theta_{12})$

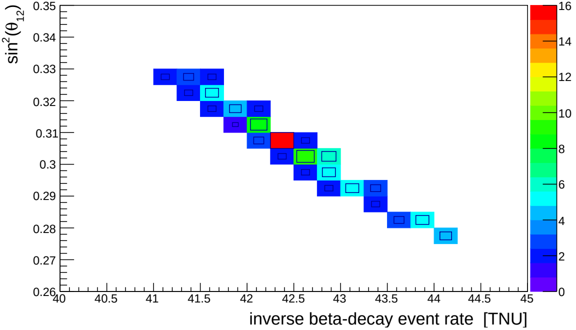

- Shown are 100 trials, random oscillation parameters sets
- Expected strong correlation: rate and $\sin^2(\theta_{12})$.
- Forero et al., PhyRev D 90 (2014): $\sin^2(\theta_{12}) = 0.323$.
- Nu-Fit 2.0, JHEP 11 (2014) 052, $\sin^2(\theta_{12}) = 0.304$
- Difference in $\sin^2(\theta_{12})$ estimate explains different rates.
- Other mixing variables with far less impact.

Scale of matter effect

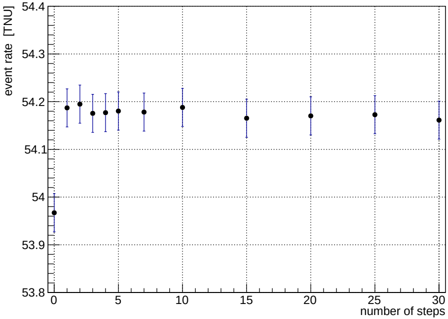

- Example arbitrary detector location, high flux region (Himalaya).
- Neutrino propagation in steps of constants electron number density.
- Zero steps is vacuum propagation (zero density).
- **Small increase** in rate of ~ 0.2 TNU or ~ 0.4 % (as expected).
- Beyond ~ 10 steps no further improvement in accuracy.

What if electron number density is higher (lower) than expected?

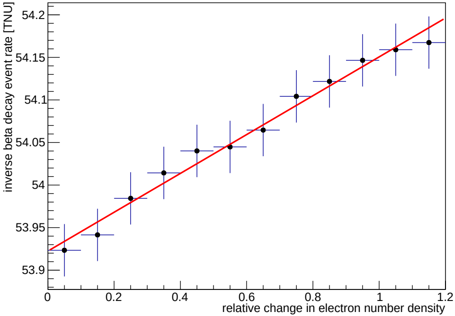

- Example arbitrary detector location, high flux region (Himalaya)
- Depending on **chemical composition** more (less) electron density, i.e. electron to nucleon ratio (Z/A) changes with hydrogen content
- Rate change of $\sim 10^{-3}$ TNU per percent in electron number density.
- Effect much smaller than present error of rate measurement.

Future prospects

Future experiments

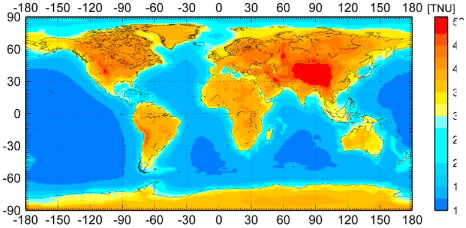

Jinping

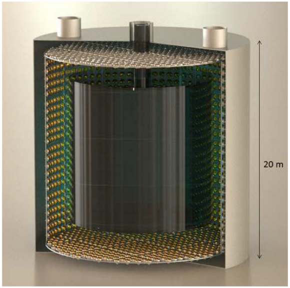

JUNO

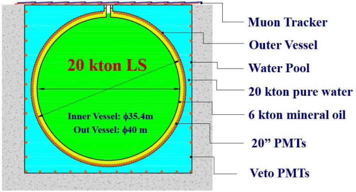

Hanohano

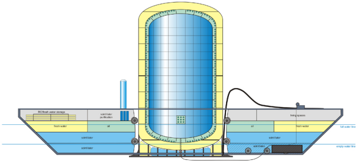

Summary

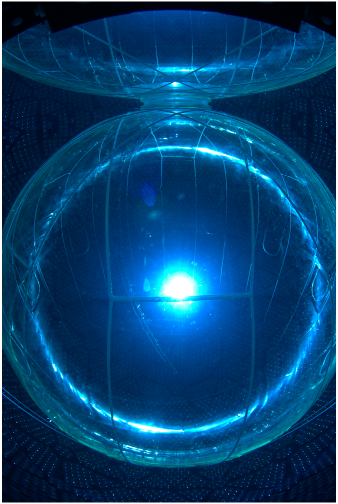

A SNO+ centric view:

- Conversion of detector to **SNO+ complete**
- Cavern and acrylic vessel water fill complete
- Scintillator fill to follow
- Expect first geoneutrino (candidate) events in 2017